Published in L. Pavesi *et al*. (eds.),
Towards the First Silicon Laser,
Kluwer Academic Publishers (2003),
pp. 209-222

OPTICAL GAIN FROM SILICON NANOCRYSTALS – A CRITICAL PERSPECTIVE

A. Polman
FOM-Institute AMOLF
Kruislaan 407, 1098 SJ Amsterdam, The Netherlands

R.G. Elliman
Department of Electronic Materials Engineering
Research School of Physical Sciences and Engineering
Australian National University, Canberra, ACT 0200, Australia

1. Introduction

It has generally been considered impossible to fabricate a silicon laser. The reason being that –due to its indirect bandgap– silicon has a small cross-section for stimulated emission. As a result, optical losses due to free carrier absorption are dominant. It has been proposed that Si nanocrystals offer a solution to this problem.

The optical properties of silicon nanocrystals are quite well understood. This is the result of extensive research over the past ten years on porous Si as well as on Si nanocrystals embedded in an SiO_2 matrix. It is generally found that well-prepared and passivated Si nanocrystals exhibit photoluminescence in the wavelength range between 500 and 1100 nm. The luminescence is attributed to the recombination of quantum-confined excitons, the emission energy thus being strongly dependent on the nanocrystal size. SiO_2 is the ideal matrix for Si nanocrystals as it can passivate dangling bonds that may cause non-radiative quenching. Indeed, many of the optical characteristics of Si nanocrystals in SiO_2 prepared by different methods, as well as oxidized porous Si, are very similar. The radiative recombination process can be entirely understood assuming a "classical" model of recombination of excitonic singlet and triplet states of the excited Si nanocrystals. In this model, the optical transition is indirect in nature, and has a relatively small cross-section.

In recent years, several applications of Si nanocrystals have been explored, and include light-emitting diodes,[1,2] non-volatile memories,[3,4] and sensitized optical amplifiers.[5,6] The fabrication of an optical amplifier or laser based on interband transitions has been considered impossible because –by analogy with bulk Si– the cross-section for free carrier absorption was thought to be higher than that for stimulated emission. Yet, in an article published in 2000, Pavesi *et al.* [7] claimed that optical gain could be achieved using Si nanocrystals, contrary to earlier predictions. Central in this claim is the presumption that the observed light

emission from silicon nanocrystals is not due to the recombination of "free" excitons but rather to the recombination of electron-hole pairs trapped at an interface state. This could, according to the authors, reduce the deleterious effect of free carrier absorption. A three-level model was introduced to explain the observed optical gain, with the intermediate level attributed to a Si=O double bond at the interface between the nanocrystal and the surrounding silicon oxide matrix.

In this paper we will first summarize recent work on the optical properties of Si nanocrystals made by ion implantation into SiO_2 thin films. These data provide extensive evidence for the "classical" excitonic model, in contrast to the surface defect model proposed by Pavesi *et al*.[7] We focus on four key issues that are important in engineering optically active Si nanocrystal assemblies: 1) passivation, 2) the homogenous and inhomogeneous line width, 3) interaction between nanocrystals, and 4) the recombination kinetics and internal quantum efficiency.

Next, we will provide experimental and theoretical arguments that the three-level Si=O defect model cannot be correct in the wavelength range at which optical gain was reported. We speculate that that optical gain could possibly be achieved in a four-level model in which the Si nanocrystals act as a sensitizer for defects or impurities in the SiO_2 host (such as e.g. Er). However, such a model does not involve quantum-confined excitons in the gain transition. We conclude that optical gain in Si nanocrystals remains an open question.

2. Optical properties of Si nanocrystals

2.1 PASSIVATION

Figure 1, taken from Min *et al*.[8] shows a photoluminescence (PL) spectrum from Si nanocrystals made using implantation of 50 keV Si ions into a thermally grown SiO_2 film on Si, at a fluence of 5×10^{16} cm^{-2}. The sample was annealed in vacuum at 1100 °C for 10 min. to induce the nucleation and growth of the nanocrystals. High-resolution transmission electron microscopy (reported in Ref. 8) shows the presence of nanocrystals with diameters ranging from 1 to 3 nm. The PL spectrum shows two broad features, peaking at 600 nm (2.1 eV) and 750 nm (1.6 eV), respectively. PL lifetime measurements at 15 K show a fast decay ($\tau<100$ ns) for the band around 600 nm, and a slow decay ($\tau=0.63$ ms) at 750 nm. The fast component for shorter wavelengths is attributed to luminescence from defect states in the glass that result from the ion implantation process. The defect luminescence originates from a very thin surface layer, as it was found to disappear after removing a 15 nm surface layer from the Si implanted film by wet etching.[9] The luminescence around 750 nm is attributed to luminescence from Si nanocrystals.

Passivation with H or D can be used to remove the defect band.[8] Figure 1(a) shows spectra after 600 eV D implantation at fluences of (0.9, 1.8, and $3.3)\times10^{15}$ cm^{-2}. As can be seen, the defect band completely disappears after D implantation. Figure 1(b) shows that after passivation, thermal annealing at 400 ºC leads to an

eight-fold increase in the PL intensity, presumably due to the in-diffusion of the D that then passivates the deeper lying Si nanocrystals. Annealing at temperatures of 500 ºC and higher reduces the passivation effect, presumably due to the out-diffusion of D. The PL lifetime remains unchanged upon the 400 ºC passivation anneal, indicating that the increase in PL is due to an increase in the density of active nanocrystals in the film. Vice versa, it indicates that samples that are not well passivated contain a large density of optically inactive nanocrystals. In such films it is impossible to achieve optical gain, as the large unbleacheable fraction of n

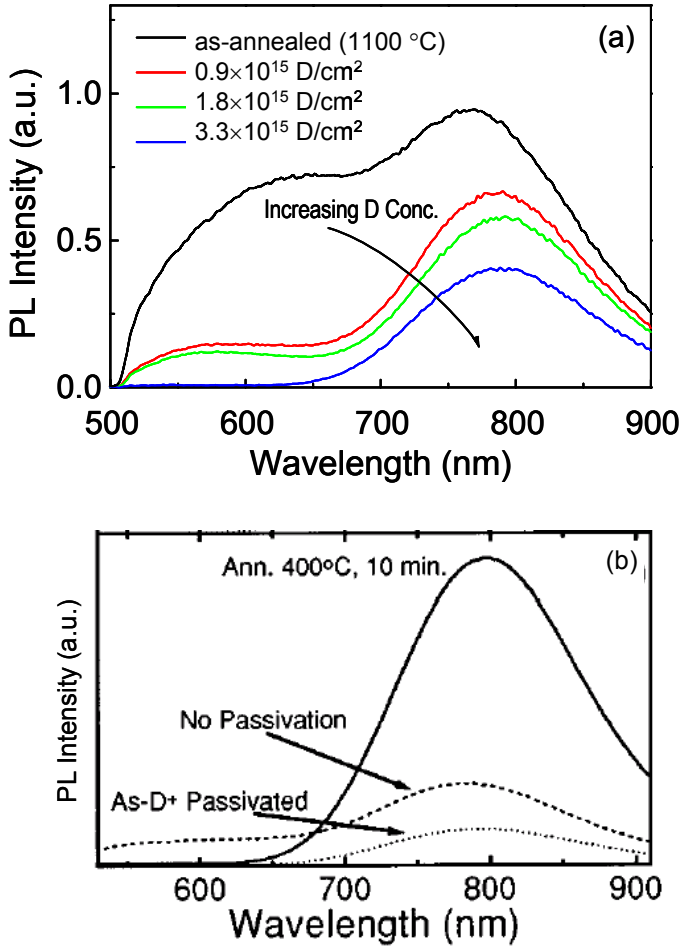

Figure 1 (a) Room temperature PL spectra of Si nanocrystal-doped SiO_2 made by 50 keV Si implantation (5×10^{16} Si/cm^2), annealed at 1100 °C for 10 min. and passivated by 600 eV deuterium implantation at (0.9, 1.8, and 3.3) $\times10^{15}$ D/cm^2. An Ar laser at 457.9 nm was used as an excitation source. (b) PL spectra before and after D passivation (same as in (a)), and after thermal annealing at 400 °C for 10 min. (From Min *et al*., Ref. 8)

2.2 HOMOGENOUS AND INHOMOGENEOUS LINEWIDTH

The luminescence feature peaking at 750 nm (1.65 eV) has a spectral width of 300 meV. The width can be partly ascribed to inhomogeneous broadening due to the large size distribution of Si nanocrystals in the film. In addition, homogeneous broadening plays a role. Recent measurements by Valenta *et al.*[10] on single nanocrystals show a homogeneous line width of 120-160 meV. A similar value is derived from phonon features in PL excitation spectra by Diener *et al.*[11] We thus conclude that the 300 meV line width of the PL spectrum for the passivated sample in Fig. 1 is due to the broad size distribution, convoluted with a ~120 meV homogeneous line width. The large homogeneous broadening can also explain the fact that sometimes PL spectra from Si nanocrystals have tails that extend well beyond the wavelength of the bandgap of bulk Si.[12] It can also partly explain the multi-exponential decay in PL lifetime measurements, as will be discussed in section 2.3.

The fact that inhomogeneous broadening plays a role firstly appears from the fact that the lifetime measured on a particular sample varies with emission wavelength. For the passivated sample in Fig. 1 it ranges from 10 μs at 650 nm to

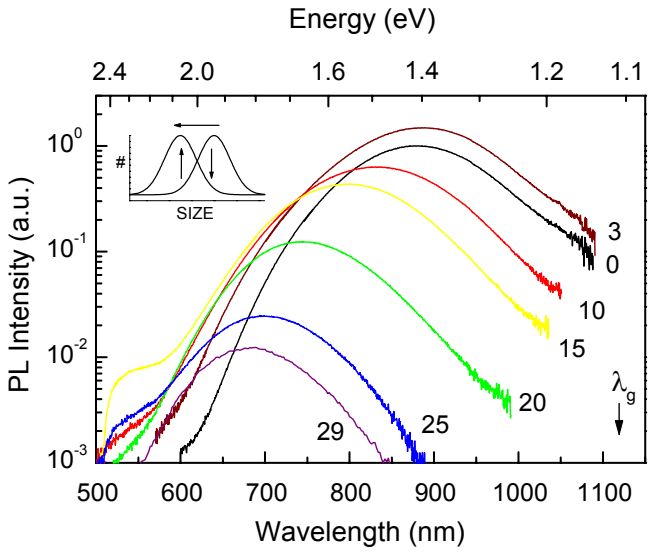

Figure 2 Room temperature PL spectra (plotted on logarithmic scale) of Si nanocrystals embedded in SiO_2 after thermal oxidation at 1000 °C in O_2 at 1 Atm., for times ranging from 0-29 min. (indicated in the figure). After oxidation, passivation was carried out using 600 eV D implantation followed by a 400 °C , 10 min. anneal. (From Brongersma *et al.*, Ref. 15)

50 μs at 850 nm.[13] The luminescence lifetime measured at 750 nm is consistent with a theoretical value for nanocrystals with a diameter of 2.5 nm.[14] The long lifetimes are characteristic for an indirect-bandgap semiconductor. The fact that the lifetimes remain long even for wavelengths as small as 500 nm indicates that even particles as small as 1 nm possess an indirect bandgap.

Given the inhomogeneous component in the spectral width it is possible to tailor the PL spectrum by tailoring the nanocrystal size distribution. For example, annealing in an oxygen ambient leads to oxidation of the Si nanocrystals, and hence a reduction of the size. This is shown in Fig. 2, which shows PL spectra (on a logarithmic scale) of samples that were annealed at 1000 ºC in 1 Atm. O_2 at times

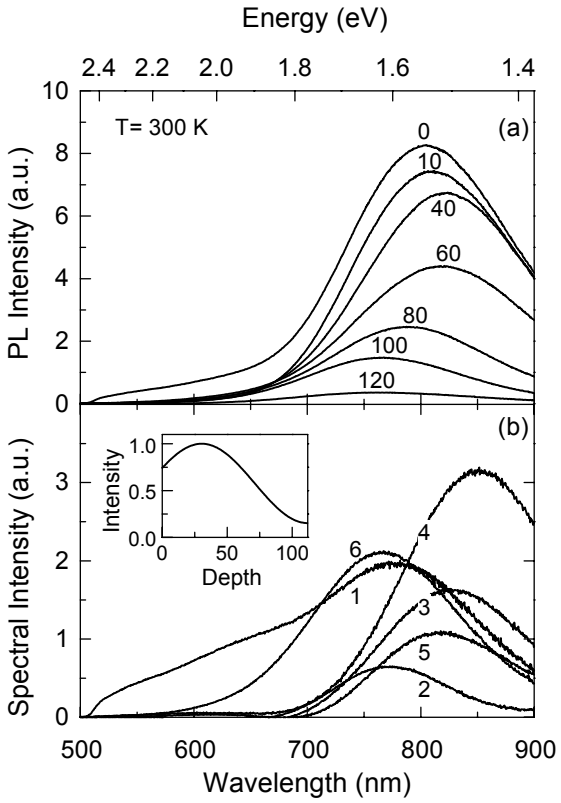

Figure 3 (a) Room temperature PL spectra obtained from a SiO_2 film containing Si nanocrystals, after etching in buffered HF for times ranging from 0 to 120 s. (b) Difference spectra obtained by subtracting spectra in (a) for subsequent etch steps, and corrected in such a way that the spectral intensity at a fixed wavelength is proportional to the average concentration of nanocrystals emitting at that wavelength. The inset shows the pump intensity profile as a function of depth in the SiO_2 film. (From Brongersma *et al.*, Ref. 9)

ranging from 3 to 29 min. (data from Brongersma *et al*., Ref. 15). The inset shows the expected change in size distribution: upon annealing the density of large nanocrystals decreases, while the density of small nanocrystals first increases. This is also seen in the PL spectra: the component at 900 nm continuously decreases with increasing oxidation time, while the signal at 600 nm first gradually increases. Using this oxidation technique the peak PL emission wavelength can be blue-shifted from 900 to 700 nm, with luminescence tails extending to 500 nm. Note that in all cases the spectral width remains in the 300–400 meV range.

Another origin of inhomogeneous broadening is the fact that the nanocrystal depth distribution is not constant throughout the thickness of the SiO_2 film.[9] First of all, this is due to the fact that Si ion implantation leads to a Gaussian depth distribution of excess Si. As the nucleation and growth rates of Si nanocrystals from a supersaturated solid solution are strongly dependent on the degree of supersaturation, the average nanocrystal size is expected to be depth dependent.

Figure 3 shows PL spectra taken after subsequent etching of a Si nanocrystal doped film in buffered HF for times ranging from 0–120 s (data from Brongersma *et al*.).[9] By subtracting the data taken after each subsequent etch and correcting for the fact that the pump beam creates a standing wave pattern leading to an inhomogeneous pump rate throughout each film, the normalized PL spectrum for each layer can be derived. It follows that small nanocrystals with emission peaking at ~750 nm are found predominantly near the surface and substrate interface, while larger nanocrystals, with emission peaking at ~ 850 nm, are found in the center of the film. The latter may be due to increased particle coarsening at high concentration, or increased interaction between nanocrystals at high concentration (see section 2.3), which leads to a spectral shift to larger wavelength. The relatively high density of small nanocrystals near the Si substrate is attributed to the effect of the substrate as a sink during precipitation.

It is important to realize that the large inhomogeneous component to the emission spectrum of Si nanocrystals (due to the size variations, both locally and a as a function of depth) will cause undesirable self-absorption and optical losses.

2.3 MULTI-EXPONENTIAL DECAY

Figure 4 shows PL decay measurement of several oxidized samples, all taken at room temperature at the same wavelength of 700 nm (from Brongersma *et al*., Ref. 15). The decay for the unoxidized sample is strongly non single-exponential. It can be fitted with a stretched exponential ($I(t)=\exp(-t/\tau)^{\beta}$) with a characteristic decay time of $\tau=12$ μs and $\beta=0.63$.[15] One explanation for this non-exponential behavior is that interaction between Si nanocrystals takes place in the highly concentrated nanocrystal-doped film, in which energy is transferred from small nanocrystals (large bandgap) to large nanocrystals (small bandgap) as indicated schematically in the inset of Fig. 4. In this way, due to the inhomogeneous distribution of nanocrystals in the film, different nanocrystals, even with the same size, can decay at different rates. Figure 4 also shows decay rates after oxidation. As can be seen,

the decay rate becomes more uniform, with τ=43 μs, and β=0.79. This is consistent with the fact that upon oxidation, the nanocrystal density and the interparticle distance increase, thus leading to reduced interaction. The nanocrystal interaction mechanism was first demonstrated to occur by Kagan *et al.*[16] for highly concentrated ensembles of CdSe quantum dots. Detailed PL decay measurements by Linnros *et al.*[17] on differently prepared Si nanocrystal ensemblies in SiO_2 made by ion implantation strongly indicate that nanocrystal interaction also takes place in that material. The interaction model is further supported by the data by Vinciguerra *et al.*[18] who found single-exponential decay in nanocrystals ensembles at low concentration.

We note that the large homogenous broadening observed for Si nanocrystals will also lead to multi-exponential decay. This is because a measurement at a fixed wavelength collects luminescence from nanocrystals with different size (within the homogeneous linewidth), and hence different decay time.

As an interesting corollary, we also note that in a thin-film system, purely single-exponential decay can never be achieved because the local optical density of states[19] is a strong function of position in the film. Calculations by De Dood *et al.*[20] show that in a 60 nm thick SiO_2 film on Si the local density of states varies by a factor 3 throughout the film. This implies that the radiative decay rate varies by a factor 3, and thus, if the quantum efficiency is high and the decay dominated by radiative decay, the integrated decay rate of excited nanocrystals distributed throughout the film thickness is not single-exponential.

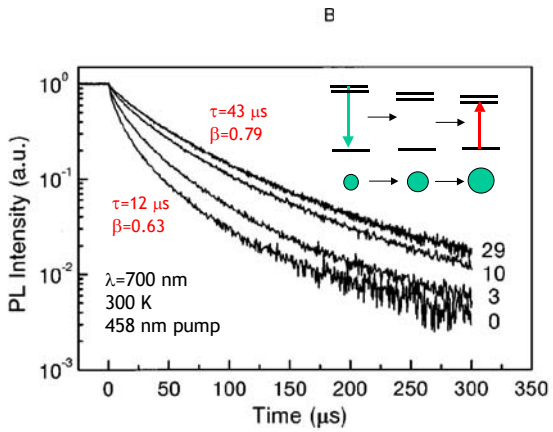

Figure 4 Normalized room temperature PL decay traces taken at 700 nm from samples oxidized at 1000 °C for 0, 3, 10, and 29 min. The inset shows a schematic of energy transfer between nanocrystals (From Brongersma *et al.*, Ref. 15)

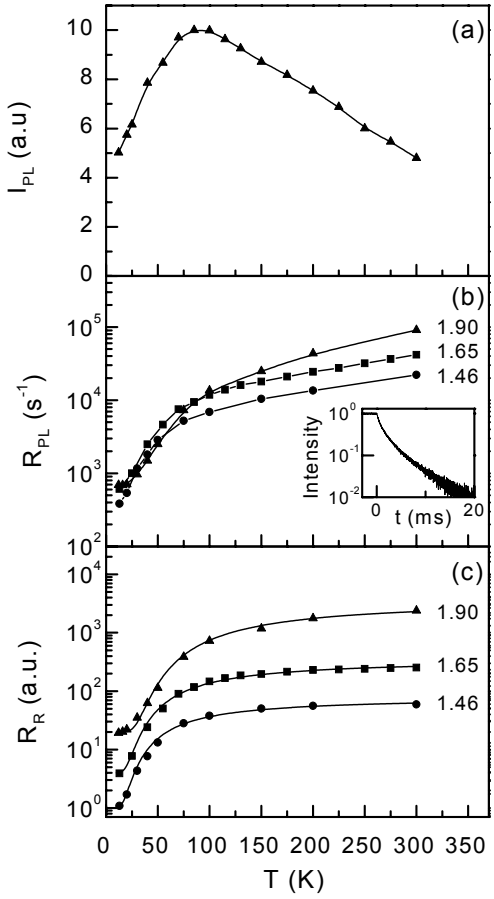

Figure 5 (a) Temperature dependence of the integrated photoluminescence intensity, I_{PL}, of Si nanocrystals in SiO_2. The solid line serves to guide the eye. (b) Temperature dependence of the photoluminescence decay rate, R_{PL}, on a logarithmic scale, measured at emission energies of 1.46 eV, 1.65 eV, and 1.90 eV. The solid lines through the data serve to guide the eye. The inset shows a typical decay trace taken at 1.65 eV and 15 K on a logarithmic intensity scale. (c) Temperature dependence of the radiative rate at emission energies of 1.46 eV, 1.65 eV, and 1.90 eV, obtained from a multiplication of the temperature dependent I_{PL} data in (a) and R_{PL} data in (b). Each data set is expressed in arbitrary units and was multiplied by a different constant factor to facilitate comparison. The solid curves are best fits of a model that takes into account the exchange splitting of the energy levels of quantum-confined excitons in the Si nanocrystals. (From Brongersma e*t al*., Ref. 13)

2.4 RECOMBINATION MODEL AND QUANTUM EFFICIENCY

The nanocrystal luminescence properties depend strongly on the temperature.[13] Figure 5(a) shows PL spectra taken at 12, 100, and 300 K, taken from Brongersma *et al*.[13] When increasing the temperature from 12 to 300 K, a 60 meV shift in the peak emission energy is seen (from 1.60 eV to 1.54 eV). This is attributed to the change in bandgap energy with temperature. For comparison: the band gap variation with temperature for bulk Si is 50 meV over the temperature range from 10 to 300 K.[21] The luminescence intensity is strongly temperature dependent, as can be seen in Fig. 5(a). As the measurements were performed in the low-pump power regime, this implies that the quantum efficiency is temperature dependent: at room temperature it is less than 50 %. It should be noted that the internal quantum efficiency is a strong function of preparation and thermal annealing conditions. For example, in samples prepared by Fujii *et al*.[22] and Kovalev *et al*.[23] it was found that the PL intensity was constant with temperature. It was noted that the cool-down time after annealing is a critical parameter determining the quantum efficiency.[24]

The luminescence lifetime is strongly temperature dependent,[13,22,25] as can be seen in Fig. 5(b). For example, at 1.65 eV it decreases from 2 ms at 10 K to 50 μs at 300 K. By multiplying the data in Fig. 5(a) and Fig. 5(b) a relative measure of the radiative decay rate can be derived at each wavelength.[13] These data are presented in Fig. 5(c) for emission energies of 1.4 eV, 1.65 eV, and 1.90 eV. At each energy, the temperature dependence of the radiative lifetime is in perfect agreement with a model for the recombination of singlet and triplet excitons, with the singlet and triplet energies split by an exchange energy, Δ, as described in Ref. 13. The ratio of singlet-to-triplet decay rates increases from 300 to 800 with increasing emission energy (decreasing nanocrystal size), as expected. It is found that Δ ranges from 8 meV at low energy to 17 meV at higher energy, in agreement with values of the exchange energy calculated using effective mass theory.[26] The value for Δ is much smaller than the 71 meV that was reported earlier for oxidized nanocrystals by Kanemitsu *et al*.[27] whose luminescence is thought to originate from states at the Si-SiO_2 interface.

2.5 SUMMARY

In summary, a detailed study of the optical properties of silicon nanocrystals shows a coherent and comprehensive picture, in which all data can be described by a model in which quantum-confined excitons recombine in Si nanocrystals with a size-dependent indirect bandgap. Important key factors to take into account when designing nanocrystal assemblies with optimized properties are:

- Luminescence from SiO_2 films containing Si nanocrystals is <u>not</u> always due to nanocrystals,
- Passivation may be required to activate “optically dead” nanocrystals that are unbleacheable under optical pumping,

- Si nanocrystals in SiO_2 show large homogeneous and inhomogeneous broadening,
- The large inhomogeneous component (due to the size distribution) causes self-absorption and optical losses,
- Multi-exponential decay is a result of: 1) interaction between nanocrystals, 2) homogeneous broadening, and 3) variation in the local optical density of states,
- The internal quantum efficiency of Si nanocrystals can be well below 100 %, depending on the annealing treatment,
- The nanocrystal recombination kinetics are very well described by the single-triplet model of quantum confined excitons,
- Si nanocrystals in SiO_2 thus behave as indirect-bandgap semiconductors, with small optical cross-sections.

None of the above analysis points at a model in which the luminescence is due to the recombination of Si=O surface states, as proposed in Ref. 7. While these important factors must be considered to optimize the optical properties of Si nanocrystals, the problem of free carrier absorption in Si nanocrystals still remains. Unless the cross-section of this effect is several orders of magnitude smaller in Si nanocrystals than in bulk Si, it will be impossible to fabricate a Si nanocrystal laser.

3. Optical gain in Si nanocrystals

In the report[7] that claimed the observation of net optical gain in Si nanocrystals an entirely new mechanism for exciton recombination in Si nanocrystals was suggested. This new claim has triggered great interest and excitement. The reported net optical gain was based on several observations:

1) Optical transmission data that showed an absorption band near 800 nm. This band was attributed to a Si surface state (Si=O double bond) that was then assigned as the initial state in the gain transition,
2) Determination of the gain cross-section from these data by comparing the measured absorbance at 800 nm with that of the nanocrystal absorbance near 500 nm, for which the cross-section was measured,
3) The proposal of a three-level model for population inversion, including the Si=O surface state,
4) A comparison of this model with theoretical results reported in the literature describing the size-dependent energy levels of Si nanocrystals with Si=O surface states,
5) Variable-stripe length measurements of the optical emission around 800 nm from the output facet of the waveguide that were fitted with an amplified spontaneous emission model,
6) Normal-incidence pump-probe measurements that showed a ~15 % change in probe intensity upon pumping a 100 nm-thick nanocrystal doped film. This

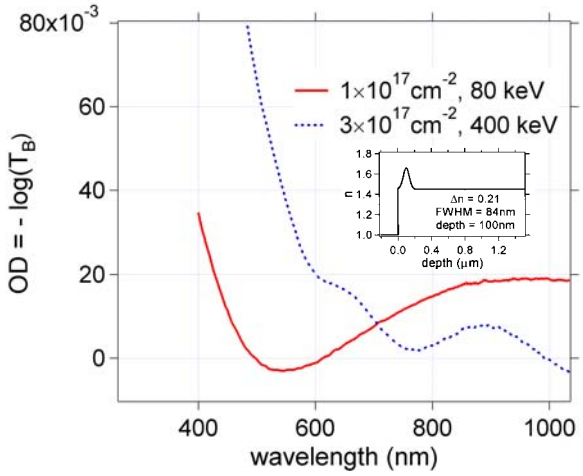

Figure 6 Optical density as a function of wavelength extracted from balanced transmission measurements for samples implanted with 80 keV (solid) and 400 keV (dashed) Si ions. The inset shows the refractive index profile for the 80 keV implant. (From Elliman et al., Ref. 28)

value was then converted to a gain coefficient of ~10^4 cm^{-1}.

In the remainder of this paper we report a critical assessment of each of these 6 observations, either by comparing with existing literature or with experiments performed in our own labs.

3.1 Si=O ABSORPTION BAND

Central in the interpretation of the data in Ref. 7 is the presumption that the observed light emission from silicon nanocrystals is not due to the recombination of "free" excitons but rather due to the recombination of electron-hole pairs trapped at an interface state. This could, according to the authors, reduce the deleterious effect of free carrier absorption, which usually prevents optical gain from indirect band gap semiconductors. The trap state was attributed to a Si=O double bond at the interface between the nanocrystal and the surrounding silicon oxide matrix.

Figure 6 shows the optical absorption data for a sample made using similar irradiation conditions as in Ref. 7 (80 keV, 1×10^{17} Si/cm^2).[28] Optical density is derived from transmission measurements assuming that changes in transmission are entirely due to absorption. This graph reproduces the data in Ref. 7. Figure 6 also shows is a measurement on a sample implanted with 400 keV Si at 3×10^{17} Si/cm^2. Interestingly, a completely different feature is now observed in the transmission measurement. Detailed analysis, reported in Ref. 28, reveals that the features observed in transmission experiments are not due to absorption, but rather to an interference effect, related to the refractive index modification created by the

Si implant (see inset in Fig. 6). All transmission data can be fitted with a simple Fresnel model for a multilayer system with multiple reflection. Thus, the existence of a Si=O state cannot be deduced from the optical absorption data in Ref. 7.

3.2 Si=O ABSORPTION CROSS-SECTION

In Ref. 7, a cross-section for stimulated emission was also derived (3×10^{-16} cm^2) from the apparent "absorption band". The finding described in section 3.1 demonstrates that this derivation is incorrect. More detailed measurements of the absorption spectrum can be performed using photo-thermal deflection spectroscopy. Figure 7 shows such spectra for the two samples in Fig. 6, taken from Ref. 28. For both samples an absorption edge is observed for smaller wavelengths, but no signature of an absorption band around 800 nm is found. From the data, an upper limit of the absorption cross-section of any transitions hidden in the noise of the measurements can be derived: 10^{-18} cm^2. This value is much too small to explain the reported optical gain.

3.3 TESTING THE THREE-LEVEL MODEL

To experimentally test the three-level model, a Si nanocrystal doped SiO_2 channel waveguide was fabricated. Note that in the previously reported[7] experiments on optical gain in Si nanocrystals a planar waveguide was employed. The advantage of a channel waveguide is that the signal mode is confined in a well-defined cross-section. In this way the pump, projected onto the sample from the top, can be accurately aligned with the waveguide. In addition, the collection geometry is

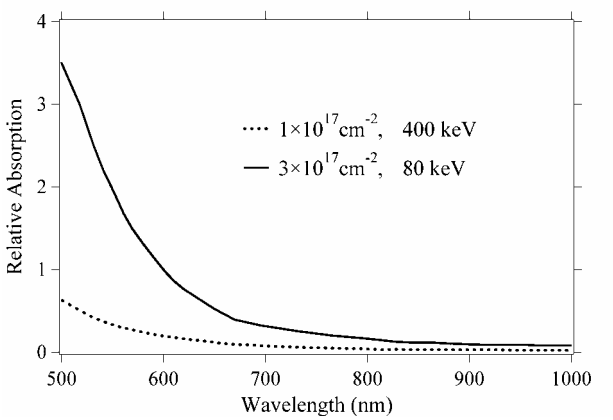

Figure 7 relative absorbance as a function of wavelength measured by photothermal deflection spectroscopy for samples implanted with 80 keV (solid) and 400 keV (dashed) Si ions. (From Elliman *et al*., Ref. 28)

better defined. Figure 8(a), taken from Kik *et al.*,[5] shows a schematic cross-section of the used waveguide geometry. An optical mode profile, measured at 1.49 μm at the output facet of the waveguide is shown in Fig. 8(b); a well-confined mode, centered on the Si nanocrystal-doped region is observed. In this particular sample the mode overlap between signal (at 1.49 μm) and Si nanocrystal doped region was 1 %. To excite the nanocrystals a continuous-wave 458 nm pump was projected onto the waveguide.[29] From measurements of the nanocrystal PL and rise time, as the pump was switched on and off, the pump rate was found to be 4×10^4 s^{-1} at 250 mW, well above the decay rate of 1.4×10^4 s^{-1} at 800 nm. Thus, assuming the simple three-level model proposed in Ref. 7, inversion should be created.

Figure 9 shows the normalized emission intensity at 850 nm coupled from the output facet of the waveguide, as a function of the length of the illuminated stripe (same technique as in Ref. 7) at two pump powers, 25 and 250 mW.[29] Except for a scaling factor of 4.6 the two curves are nearly identical. In the variable-stripe-length method, the emission intensity $I(l)$ as function of illumination length l is then given by:

$$I(l) = (I_{spont} / (g-\alpha)) \times (e^{(g-\alpha)l} - 1) \qquad (1)$$

with I_{spont} the spontaneous emission intensity, g the gain, and α the overall waveguide loss, all defined per unit length.[30] Eqn. (1) fits the data very well, and we find $(g-\alpha) \approx -10$ cm^{-1} for both pump powers.[31] This demonstrates that g=0 and that the behavior in Fig. 9 is entirely due to waveguide loss: $\alpha \approx 10$ cm^{-1}. As no optical gain is observed we thus demonstrate that the simple three-level model is incorrect and that it should be modified either to include non-linear processes under high-intensity pumping, or should be replaced by a four-level model.[32] For example, optical gain could possibly be achieved in a four-level model in which the Si nanocrystals act as a sensitizer for defects or impurities in the SiO_2 host.

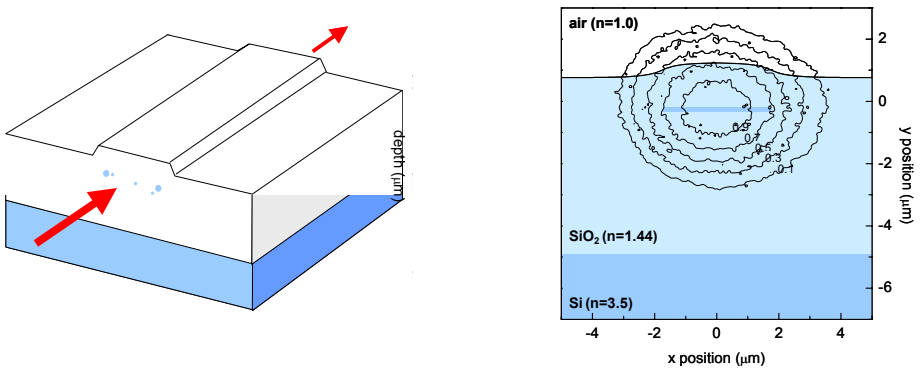

Figure 8 (a) Schematic of Si nanocrystal doped SiO_2 channel waveguide. (Right) Optical mode image at λ=1.49 μm measured at the output facet of the waveguide. (From Kik *et al.*, Ref. 5)

3.4 COMPARING THE Si=O THREE-LEVEL MODEL WITH LITERATURE

The proposal for a Si surface state related model was carefully compared with the theory by Wolkin *et al*.[33] This model predicts that for nanocrystals emitting at 800 nm (the wavelength at which optical gain was reported), the emission is not due to a trap state, but rather due to recombination of quantum-confined excitons centered in the nanocrystals. In this model, a three-level model was only found for wavelengths < ~640 nm; a four level model was found for wavelengths < ~500 nm. These wavelengths are much different to those for which gain was reported.

3.5 VARIABLE-STRIPE LENGTH MEASUREMENTS AND CORRECTIONS

Recent literature[34] demonstrates that the use of the variable-stripe method is sensitive to several artifacts. First of all, diffraction of the pump beam from the slit will create an inhomogeneous intensity profile on the illuminated section of the

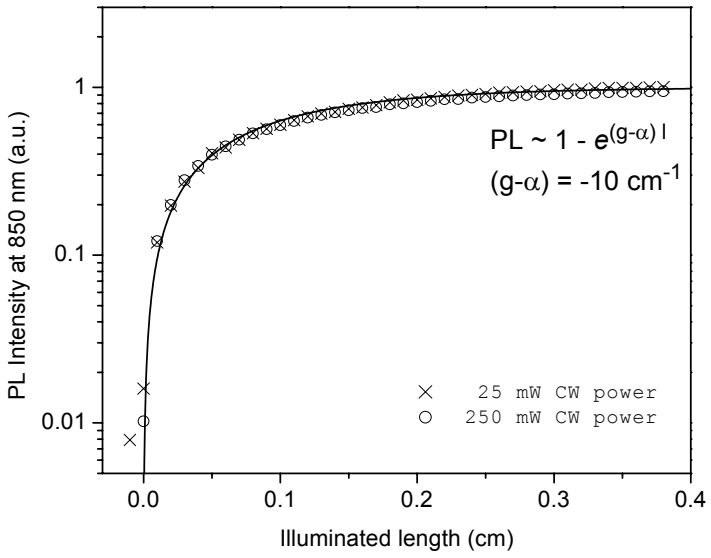

Figure 9 Normalized optical emission intensity at 850 nm from a Si nanocrystal doped waveguide (1×10^{17} Si/cm^2), as a function of illuminated length (pump wavelength 458 nm). The pump stripe geometry was the same as in Ref. 7. We attribute the data point for the shortest length to an artifact, e.g. the improper definition of length (for short length) and/or scattering of pump light. (From Kik *et al*., Ref. 29)

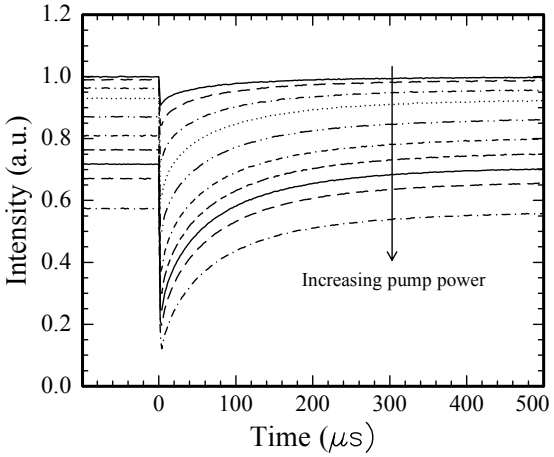

Figure 10 Time dependence of the normalized 800 nm probe intensity measured on exit from the waveguide, measured after excitation with a 25 ns pulse at 355 nm (at t=0). Curves from top-to-bottom correspond to pump energy densities of 3.5, 7.0, 15.5, 35, 70, 175, 350, 700, 1750 and 3500 μJ/cm^2, respectively. From Elliman *et al.*, Ref. 35)

waveguide. Second, a confocal effect takes place, in which the collection efficiency of light emitted from the waveguide is not constant over the length of the waveguide, but depends on the position of the focus of the collecting microscope objective. The challenge in performing variable-stripe measurements now lies in clear partitioning of 1) raw measured data, 2) precise determination of correction factors and their error bars, including at least diffraction and confocal effects, 3) correction of the raw data, and determination of their error bars, 4) fitting Eqn. (1) to the corrected data.

3.6 PUMP-PROBE EXPERIMENTS IN WAVEGUIDE GEOMETRY

Improved pump-probe experiments were undertaken to verify the results reported in Ref. 7. Instead of using a transmission geometry, which restricts the interaction length to the thickness of the implant distribution (~100 nm in the case of Ref. 1), an 800-nm probe beam was coupled into a ~2 cm long Si nanocrystal-doped planar waveguide.[35] The waveguide was made by implanting a 12 μm thick thermal SiO_2 layer (thermally grown on Si) with 600 keV Si ions to a fluence of 2.6×10^{17} cm^{-2}. Nanocrystals were then formed by annealing at 1100 °C (1 hr. in N_2). The guided beam propagated ~15 mm in the waveguide before emerging from the edge of the cleaved sample where its intensity was measured using a Si photodiode. A 2.5 mm section of the guided beam was irradiated with a 355 nm pump beam having a pulse width (FWHM) of 25 ns and a repetition rate of 30 Hz. The time response of the probe signal was monitored following each pump pulse and studied as a function pump energy density (3.5-3500 μJ/cm^2).

Figure 10, taken from Ref. 35, shows time-dependent measurements of the

probe output following the pump pulse. The data clearly show that the probe beam is attenuated by the pump and that the attenuation increases with increasing pump power – no evidence for optical gain was observed. The recovery of the probe signal is also evident, occurring on a time scale of 45-70 μs (depending on the pump power); a value similar to the PL lifetime of nanocrystals at 300 K. This suggests that the observed transient absorption is related to an excited-state absorption process such as free-carrier absorption. Whilst these are preliminary measurements they suggest that –similarly to bulk Si– free-carrier absorption could be a major limiting factor that prohibits the achievement of optical gain in Si nanocrystals.

Finally we mention measurements by Mimura et al.,[36] who have measured the infrared optical absorption spectra of P-doped Si nanocrystals. They attributed the measured absorption tails to intervalley transitions of free electrons supplied by the P dopants. The (extrapolated) absorption coefficient due to free carrier absorption around 800 nm was found to be $\sim 10^2$ cm^{-1} for highly doped nanocrystals.

4. Conclusions

The optical properties of Si nanocrystals made using Si ion implantation into SiO_2, and subsequent annealing, are quite well understood. The broad range of data presented in the first section of this paper was shown to be consistent with a model in which quantum-confined excitons recombine in Si nanocrystals with an indirect bandgap that varies with nanocrystal size. From these data it is evident that key factors of importance for the design of nanocrystal assemblies with optimized luminescence properties are: 1) passivation, 2) homogeneous and inhomogeneous broadening, 3) interaction between nanocrystals, and 4) the luminescence quantum efficiency. Si nanocrystals in SiO_2 behave as indirect-bandgap semiconductors, with small optical cross-sections.

The report by Pavesi *et al.*[7] that claimed the observation of net optical gain in Si nanocrystals is very intriguing. A critical assessment of each of the six observations made in the paper was presented. We conclude that the proposed simple three-level mode is incorrect. We speculate that optical gain could possibly be achieved in a material in which the Si nanocrystals act as a sensitizer for defects or impurities in the SiO_2 host (such as e.g. Er). However, such a model does not involve quantum-confined excitons in the gain transition. More detailed measurements of the variable-stripe technique are required to evaluate data taken using this technique. Pump-probe measurements on planar waveguides show no gain, but instead a transient enhanced absorption, possibly due to free carrier absorption. We conclude that optical gain from silicon nanocrystals remains an open question.

Acknowledgements

This work is part of the research program of the Foundation for Fundamental Research on Matter (FOM) and is financially supported by the Dutch Organization for the Advancement of Science (NWO). We gratefully acknowledge the contri-

butions of our co-workers. They are listed in the references quoted in the captions.

References

[1] P. Photopoulos and A. G. Nassiopoulou, Appl. Phys. Lett. **77**, 1816 (2000).
[2] A. Irrera, D. Pacifici, M. Miritello, G. Franzò, F. Priolo, F. Iacona, D. Sanfilippo, G. Di Stefano, and P.G. Fallica, Appl. Phys. Lett. **81**, 1866 (2002).
[3] S. Tiwari, F. Rana, H. Hanafi, A. Hartstein, and E.F. Crabbé, Appl. Phys. Lett. **68**, 1377 (1996).
[4] M.L. Ostraat, J.W. De Blauwe, M.L. Green, L.D. Bell, M.L. Brongersma, J. Casperson, R.C. Flagan, and H. A. Atwater, Appl. Phys. Lett. **79**, 433 (2001).
[5] P.G. Kik and A. Polman, J. Appl. Phys. **91**, 534 (2002).
[6] H.-S. Han, S.-Y. Seo, and J.H. Shin, Appl. Phys. Lett. **79**, 4568 (2002).
[7] L. Pavesi, L. Dal Negro, C. Mazzoleni, G. Franzò, and F. Priolo, Nature **408**, 440 (2000).
[8] K.S. Min, K.V. Shcheglov, C.M. Yang, H.A. Atwater, M.L. Brongersma, and A. Polman, Appl. Phys. Lett. **69**, 2033 (1996).
[9] M.L. Brongersma, A. Polman, K.S. Min, and H.A. Atwater, J. Appl. Phys. **86**, 759 (1999).
[10] J. Valenta, I. Pelant, and J. Linnros, Appl. Phys. Lett. **81**, 1398 (2002).
[11] J. Diener, D. Kovalev, H. Heckler, G. Polisski, and F. Koch, Phys. Rev. B. **63**, 73302 (2001).
[12] F. Priolo, G. Franzò, D. Pacifici, V. Vinciguerra, F. Iacona, and A. Irrera, J. Appl. Phys. **89**, 264 (2001).
[13] M.L. Brongersma, P.G. Kik, A. Polman, K.S. Min, and H.A. Atwater, Appl. Phys. Lett. **76**, 351 (2000).
[14] M. Hybertsen, Phys. Rev. Lett. **72**, 1514 (1994).
[15] M.L. Brongersma, A. Polman, K.S. Min, E. Boer, T. Tambo, and H.A. Atwater, Appl. Phys. Lett. **72**, 2577 (1998).
[16] C. R. Kagan, C. B. Murray, M. Nirmal, and M. G. Bawendi, Phys. Rev. Lett. **76**, 1517 (1996).
[17] J. Linnros, N. Lalic, A. Galeckas, and V. Grivickas, J. Appl. Phys. **86**, 6128 (1999).
[18] V. Vinciguerra, G. Franzò, F. Priolo, F. Iacona, and C. Spinella, J. Appl. Phys. **87**, 8165 (2000).
[19] E. Snoeks, A. Lagendijk, and A. Polman, Phys. Rev. Lett. **74**, 2459 (1995).
[20] M.J.A. de Dood, L.H. Slooff, A. Moroz, A. van Blaaderen, and A. Polman, Phys. Rev. A. **64**, 33807 (2001), P.G. Kik, "Energy transfer in erbium doped optical waveguides based on silicon", Ph.D. Thesis, FOM-Institute AMOLF (2000), p. 102.
[21] S.M. Sze, *Physics of semiconductor devices* (John Wiley and Sons, New York, 1981).
[22] S. Takeoka, M. Fujii, and S. Hayashi, Phys. Rev. B **62** 16820 (2000).
[23] D. Kovalev, private communication (2002).
[24] M. Fujii, private communication (2002).
[25] J. Diener, D.I. Kovalev, G. Polliski, and F. Koch, Appl. Phys. Lett. **74**, 3350 (1999).
[26] P.D.J. Calcott *et al.*, J. Phys. Cond. Matt. **5**, L91 (1993).
[27] Y. Kanemitsu, Phys. Rev. B **53**, 13515 (1996).
[28] R.G. Elliman, M.J. Lederer, and B. Luther-Davies, Appl. Phys. Lett. **80**, 197 (2002).
[29] P.G. Kik, M.J.A. de Dood, and A. Polman, to be published.
[30] Note that Eqn. (1) deviates from Eqn. (1) in Ref. 7, in that it does not include the linear term *l* in the prefactor, see: K.L. Shaklee, R.E. Nahaory, and R.F. Leheney, J. Lumin. **7**, 284 (1973).
[31] We note that, as discussed in section 3.5, variable-stripe length methods are sensitive to artifacts due to diffraction and confocal effects. The data by Kik *et al.* presented here are

not corrected for such effects. However, the fact that similar curves are found for low and high pump power is a strong indication that no optical gain is observed.

[32] A. Polman, presented at the MRS Fall Meeting, Boston, November, 2001.

[33] M.V. Wolkin, J. Jorne, P.M. Fauchet, G. Allan, and C. Delerue, Phys. Rev. Lett. **82**, 197 (1999).

[34] J. Valenta, I. Pelant, and J. Linnros, Appl. Phys. Lett. **81**, 1398 (2002).

[35] R.G. Elliman, M.J. Lederer, N. Smith, and B. Luther-Davies, presented at 13th International Conference on Ion Beam Modification of Materials, Kobe, Japan, September 1-6, 2002, to be published in Nucl. Instr. and Meth. B (2003).

[36] A. Mimura, M. Fujii, S. Hayashi, D. Kovalev, and F. Koch, Phys. Rev. B. **62**, 12625 (2000).